Manaaki Whenua
Landcare Research

Planning soil conservation for sediment load reduction in Taranaki

Prepared for: Taranaki Regional Council

March 2021

Planning soil conservation for sediment load reduction in Taranaki

Contract Report: LC3942

Andrew Neverman, Hugh Smith, Alexander Herzig

Manaaki Whenua – Landcare Research

Reviewed by:	*Approved for release by:*
Chris Phillips	Chris Phillips
Portfolio Leader – Managing Land & Water	Portfolio Leader – Managing Land & Water
Manaaki Whenua – Landcare Research	Manaaki Whenua – Landcare Research

Disclaimer

This report has been prepared by Manaaki Whenua – Landcare Research for Taranaki Regional Council. If used by other parties, no warranty or representation is given as to its accuracy and no liability is accepted for loss or damage arising directly or indirectly from reliance on the information in it.

Contents

Summary v
1 Introduction 1
2 Background 1
3 Objectives 2
4 Methods 2
4.1 SedNetNZ Model Description 2
4.2 Model simulations 11
4.3 Contemporary and achievable attribute states 14
5 Results 16
5.1 Scenario mean annual suspended sediment loads 16
5.2 Reductions in load 18
5.3 Suspended sediment attribute states 20
5.4 Achievement of NPS-FM 2020 suspended sediment attribute states 22
6 Discussion 23
6.1 Effectiveness of soil conservation works 23
6.2 Attribute bands 24
6.3 Model assumptions and limitations 26
7 Conclusions 29
8 Recommendations 29
9 Acknowledgements 30
10 References 30

Summary

Project and Client

- Taranaki Regional Council (TRC) contracted Manaaki Whenua – Landcare Research (MWLR) to model mean annual suspended sediment loads and the reductions in load required to meet the suspended fine sediment attribute states (visual clarity) in the National Policy Statement for Freshwater Management 2020 amendment (NPS-FM 2020). This modelling will contribute to soil conservation planning to meet future water quality targets in the Taranaki region.

Objectives

- Model mean annual suspended sediment loads using SedNetNZ for:
  - a landcover scenario representing a pre-mitigation state.
  - a landcover scenario representing the contemporary state.
  - a landcover scenario representing a future state under best practice soil conservation works.
- Assess the sediment load reduction achieved by soil conservation works implemented to date.
- Establish baseline visual clarity at water quality monitoring sites across the region.
- Model the reductions in contemporary mean annual suspended sediment loads required to achieve the national bottom line and A-C attribute states for fine suspended sediment in the NPS-FM 2020.
- Assess the feasibility of achieving the national bottom line and A-C attribute states under the best practice soil conservation scenario and provide a ranked list of priority REC2 sub-catchments to target for soil conservation works.

Methods

- Mean annual suspended sediment loads were modelled for a nominal year of 1996 to represent sediment loads before soil conservation works. Landcover for this period was represented by the New Zealand Landcover Database version 1 (LCDBv1), EcoSat Woody, and existing riparian fencing.
- A second scenario was modelled using LCDBv5, existing Whole Farm Plans and their contemporary maturity, and the contemporary extent of riparian fencing. This scenario represents contemporary mean annual suspended sediment loads, with a nominal year of 2018.
- A final scenario was modelled with WFPs fully matured, and a completed extent of riparian fencing. This scenario represents the load reductions achievable given full implementation and maturity of best practice soil conservation works in Taranaki, and can be used to assess the feasibility of achieving fine suspended sediment attribute states in the NPS-FM 2020. Full maturity could be achieved by 2035.
- Monthly visual clarity monitoring data were compiled for 14 water quality monitoring sites across the Taranaki region and used to calculate the median visual clarity for the

past 5 years to establish a baseline visual clarity. 5 years is the minimum period for baseline calculation in the NPS-FM 2020.

- The mean annual suspended sediment load reductions required to achieve higher visual clarity attribute states were calculated using national-scale empirical models of the relationship between SSC and visual clarity.

Results

- Modelled mean annual suspended sediment loads for the Taranaki region were 2.38 Mt yr^{-1} for the initial baseline scenario, reducing to 1.68 Mt yr^{-1} for the contemporary scenario. Future loads are expected to be 1.44 Mt yr^{-1} for the region under current landcover with full implementation and maturity of soil conservation works.
- Despite some land cover change leading to local increases in soil erosion, SedNetNZ modelling for the Taranaki region suggests soil conservation works implemented since ~1996 have resulted in a 29% net reduction in mean annual suspended sediment loads across the region. As existing soil conservation works mature, and further riparian fencing is completed, a further 15% reduction is expected across the region under the current landcover configuration.
- The NPS-FM 2020 sets 5 classes for suspended sediment: bands A, B, and C which represent acceptable levels of fine sediment, with band A being the best, a national bottom line, which is the minimum acceptable standard, and band D which is below the minimum acceptable level. Based on the past 5 years of monthly water quality monitoring data from 14 sites across the region, seven of the 14 sites presently sit in band A for visual clarity in the NPS-FM 2020. This is the highest achievable attribute state for fine suspended sediment, and represents a state where suspended sediment has a minimal impact on instream biota, and ecological communities are similar to those observed in natural reference conditions.
- Of the remaining seven sites, four sites have a state better than the national bottom line, two of which achieve band B status, and two achieve band C. Eleven of the 14 sites are therefore above the national bottom line and require no further reductions in suspended sediment. Three sites presently fall below the national bottom line.

Conclusions and Recommendations

- Soil conservation works implemented since ~1996 have resulted in an estimated 29% net reduction in mean annual suspended sediment loads across the region. A further 15% reduction is expected across the region under the current landcover configuration as existing soil conservation works mature and riparian fencing is completed. This state would be achieved as early as 2035 under this SedNetNZ model configuration.
- Seven of the 14 sites analysed presently sit in band A for visual clarity in the NPS-FM 2020. This is the highest achievable attribute state. Two sites are in band B, and two in band C, totalling 11 sites sitting above the national bottom line, and therefore requiring no further reduction. Three sites presently sit below the national bottom line.
- Uncertainty about the present maturity of existing soil conservation works likely means the model has underestimated the sediment load reductions that can be

achieved in the future. This modelling could be improved with comprehensive data on the present level of completion of soil conservation in Whole Farm Plans, and their maturity.

- The availability of regional LiDAR data will enable better representation of erosion processes within SedNetNZ. Future work could update SedNetNZ modelling for the region when LiDAR data become available.
- Climate change is likely to have an adverse effect on suspended sediment loads and may offset the reductions achieved by soil conservation works by the end of the century. SedNetNZ modelling could be undertaken for the Taranaki region to explore the potential impact of climate change on mean annual suspended sediment loads.

1 Introduction

To achieve national freshwater targets, erosion and sediment control practices and/or land management change are required to reduce sediment loads and improve visual clarity (Neverman et al. 2019). Taranaki Regional Council (TRC) contracted Manaaki Whenua – Landcare Research (MWLR) to use spatial modelling to 1) identify monitoring catchments requiring reductions in suspended sediment loads to achieve the range of attribute states for suspended fine sediment in the NPS-FM 2020, and 2) identify and prioritise areas within these catchments for soil conservation and erosion control work.

SedNetNZ (Dymond et al. 2016) was identified as the most appropriate model for these objectives. SedNetNZ is a steady-state sediment budget model designed to represent the diversity of erosion processes that occur in the New Zealand landscape and predict mean annual suspended sediment yields (Dymond et al. 2016). Recent updates to the SedNetNZ model include improved representation of streambank erosion (Smith et al. 2019) as well as spatial variability in surface soil erodibility and lake trapping of suspended sediment (Neverman et al. 2020). SedNetNZ represents erosion processes individually, allowing direct targeting of erosion processes with appropriate mitigations during mitigation scenario modelling. This improves on the national-scale modelling framework employed by Neverman et al. (2019), which utilised the NZeem model (Dymond et al. 2010) that does not represent individual erosion processes.

2 Background

In 2020 the Ministry for the Environment (MfE) amended the National Policy Statement for Freshwater Management (NPS-FM) and National Objectives Framework (NOF). The NPS-FM and NOF require a minimum standard to be achieved (a national bottom line) for water quality attributes, along with a requirement for no further degradation for water bodies which already exceed the national bottom line. Councils are required to develop plans to achieve these standards.

Previous versions of the National Policy Statement for Freshwater Management (NPS-FM 2014 and 2017) did not include limits for fine suspended sediment. Following the 2017 amendment, MfE led work to develop a fine suspended sediment attribute (Franklin et al. 2019; Hicks et al. 2019; Neverman et al. 2019). This work resulted in the inclusion of a fine suspended sediment attribute in the 2020 amendment to the NPS-FM, with attribute states set using visual clarity targets.

Taranaki Regional Council engaged Manaaki Whenua – Landcare Research (MWLR) to provide modelled mean annual suspended sediment loads under a set of scenarios to explore the suspended sediment load reductions achieved by soil conservation works to date, and to assess the feasibility of achieving NPS-FM 2020 fine suspended sediment attribute states at water quality monitoring sites throughout the region through prioritised soil conservation works.

Dymond et al. (2017) identified relationships between suspended sediment concentration and visual clarity and turbidity. Hicks et al. (2019) used these relationships to develop

nationally fitted models to predict the reductions required in mean annual suspended sediment loads to achieve visual clarity and turbidity bottom lines. Following a similar approach to Neverman et al. (2019), these models have been applied to estimate the reductions in the SedNetNZ baseline mean annual suspended sediment loads required to achieve the NPS-FM 2020 fine suspended sediment attribute states at water quality monitoring sites across Taranaki.

3 Objectives

- Model mean annual suspended sediment loads using SedNetNZ for:
  - a landcover scenario representing a pre-mitigation state.
  - a landcover scenario representing the contemporary state.
  - a landcover scenario representing a future state under best practice soil conservation works.
- Assess the sediment load reduction achieved by soil conservation works implemented to date.
- Establish baseline visual clarity at water quality monitoring sites across the region.
- Model the reductions in contemporary mean annual suspended sediment loads required to achieve the national bottom line and A-C attribute states for fine suspended sediment in the NPS-FM 2020.
- Assess the feasibility of achieving the national bottom line and A-C attribute states under the best practice soil conservation scenario, and provide a ranked list of priority REC2 sub-catchments and farms to target for soil conservation works.

4 Methods

4.1 SedNetNZ Model Description

4.1.1 Surficial Erosion

Surficial erosion processes in SedNetNZ (Dymond et al. 2016) are represented by the NZUSLE (Dymond 2010) model:

$$ES = a\,P^2KLSC \quad (1)$$

where ES denotes surficial erosion in t km^{-2} yr^{-1}; a is a constant (t km^{-2} yr^{-1} mm^{-2}) calibrated against measurements (Dymond 2010) with a value of 1.2 x 10^{-3}; P is mean annual rainfall (mm); K is the soil erodibility factor (dimensionless), L is the slope length factor, estimated as $\left(\frac{\lambda}{22}\right)^{0.5}$ with λ assumed globally = 200 m; S is the slope steepness factor, estimated by 0.065 + 4.56 θ + 65.41 θ^2, where θ denotes the dimensionless slope gradient; and C represents the impact of vegetation cover (dimensionless) (1.0 for bare ground, 0.01 for pasture, and 0.005 for forest and scrub).

In this study, we use a revised representation of surficial erosion processes as part of the SedNetNZ model. Following Smith et al. (2019b), this includes replacing the uniform slope length factor (*L*) of the NZUSLE (Dymond 2010) with a factor that better represents the effect of topography on the size of convergent upslope areas contributing overland flow and surficial erosion, as described by Desmet and Govers (1996):

$$L = \frac{(A + D^2)^{m+1} - A^{m+1}}{D^{m+2} * x^m * 22.13^m} \quad (2)$$

where L is slope length factor for a given raster cell (pixel), A is the upstream catchment area (m^2) at the cell inlet, D is the raster cell width (m), m is the slope length exponent, $x = \sin a + \cos a$, with α being the slope aspect.

The slope length exponent m is calculated depending on the rill to inter-rill ratio β and the slope gradient θ (Foster et al. 1977 and McCool et al. 1989, cited in Renard et al. 1997):

$$\beta = \frac{\frac{\sin\theta}{0.0896}}{3 * (\sin\theta)^{0.8} + 0.56} \quad (3)$$

$$m = \frac{\beta}{1 + \beta} \quad (4)$$

We also apply a revised slope factor, S, which is calculated according to a threshold in slope gradient sp (%) (Renard et al. 1997):

$$S = \begin{cases} 10.8 * \sin\theta + 0.03 & with\ sp < 9\% \\ 16.8 * \sin\theta - 0.5 & with\ sp \geq 9\% \end{cases} \quad (5)$$

Furthermore, we apply a revised, spatially–variable, *K* factor in the NZUSLE developed in Neverman et al. (2020) to better represent the spatial variability of soil erodibility, utilising the Fundamental Soils Layer (FSL) to represent soil parameters. We adapted the *K* factor equations in Wang et al. (2001) and Yang et al. (2018) to the NZUSLE:

$$K = \frac{2.1(12 - OM)M^{1.14}10^{-4} + 3.25(SS - 2) + 2.5(PP - 3)}{7.59\ x\ 10} \quad (6)$$

where *OM* is the soil organic matter content, *M* is the particle size parameter, *SS* is the soil structure code, and *PP* is the soil profile permeability code. We use 6 *PP* classes, adapted from Rosewell & Loch (2002). The soil structure code was set at *SS* = 2 as the FSL has insufficient data on soil structure to relate to the *SS* classes used for calculating *K*. We found the magnitude of *K* was not sensitive to the choice of *SS* class value. *M* is calculated as a function of the proportion silt and clay:

$$M = Silt(100 - Clay) \quad (7)$$

where *Silt* and *Clay* are the percent of silt and clay in the soil, respectively.

Silt was limited to a range of 15–70%, and *OM* was capped at 4% to fit the nomograph of Wischmeier et al. (1971) used to derive Equation 6 for organic soils.

4.1.2 Shallow Landslide Erosion

Shallow landslides are considered to be the most common form of erosion In New Zealand hill country (Eyles 1983). Typical landslides are seldom greater than 2 m deep, and individual failures are usually of small areal extent (50–100 m^2) (Smith et al. 2021). They usually have a debris tail of deposited sediment below their source that often reaches a stream (for approximately half of debris tails – Dymond et al. 1999). Landslide occurrence is highly correlated with slope angle, with most failures occurring on slopes steeper than 26 degrees, but landslides can occur on slopes as low as 15 degrees (DeRose 2013; Smith et al. 2021). The expected mass of soil lost to landslide erosion per square kilometre per year, and the connection with a stream, is given by *EL*:

$$EL = \rho \, SDR \, d_l \, f(s) \tag{8}$$

where ρ is the bulk density of soil (t m^{-3}), *SDR* is the sediment delivery ratio, d_l is the mean depth of landslide failure (m), and *f(s)* is the expected area of landslide scars per square kilometre per year at slope angle s (m^2 km^{-2} a^{-1}).

Landslide erosion is estimated for those Erosion Terrains[1] (see Dymond et al. 2010) identified as being susceptible to landslide erosion. ρ is set to 1.5 t m^{-3} (Dymond et al. 2016); *SDR* is set to 0.5 for hill country and 0.1 for mountainland (Dymond et al. 2016); d_l is set to 1 m (Page et al. 1994; Reid & Page 2003); and *f(s)* is determined from previous calibration of SedNetNZ in the Manawatu (Dymond et al. 2016; Betts et al. 2017) and adjusted for the Taranaki region using information on storm rainfall magnitude-frequency (NIWA HIRDS v4) and estimated landslide triggering rainfall thresholds (Basher et al. 2020).

4.1.3 Earthflow erosion

Slow-moving earthflows (c. 1 m per year) are common in Erosion Terrains underlain by crushed mudstone and argillite (Dymond et al. 2010). The delivery of sediment to streams is via the undercutting of earthflow toes. The mass of soil delivered to streams by earthflows in t km^{-2} a^{-1} is denoted by *EE* and is estimated as:

$$EE = \rho \, d_e \, v \, ED \tag{9}$$

Where ρ is the bulk density of soil (t m^{-3}), d_e is the mean depth of earthflows (m), v is the mean speed of earthflows (m a^{-1}), and *ED* is the mean length of stream intersecting earthflow toes in a square kilometre (m km^{-2}).

ρ is set to 1.5 t m^3 (Dymond et al. 2016); d_e is set to 3 m (through field observation (Dymond et al. 2016)); and v is set to 0.1 m a^{-1} (average from published data — Guy 1977;

[1] An erosion terrain is a land type with a unique combination of erosion processes and rates leading to characteristic sediment generation and yields. Erosion terrains were derived from New Zealand Land Resource Inventory data and are based on combinations of rock type/parent material, topography, rainfall, and erosion process type and severity. Erosion terrains coefficients are listed in Dymond et al. (2010).

Zhang et al. 1991; Marden et al. 2008, 2014). *ED* is set to 1,024 m km^{-2} (from digitising stream lengths on digitised aerial photographs – Dymond et al. 2016).

4.1.4 Gully erosion

Gullies commonly initiate at channel heads, usually as a result of excessive surface or subsurface water flow. Once initiated, a gully can continue to expand over long time periods (decades). The mass of soil delivered to streams by gullies, in t km^{-2} a^{-1}, is denoted by *EG* and is estimated by:

$$EG = \rho\ Ag\ GDT \tag{10}$$

where ρ is the bulk density of soil (t m^{-3}), A_g is the mean cross-sectional area of gullies (m^2), *GD* is the length of gullies in a square kilometre (m km^{-2}), and *T* is the time since gully initiation (yr).

Using the methodology outlined in Dymond et al. (2016): ρ is set to 1.5 t m^{-3}; A_g is set to 900 m^2 (from field observations); *GD* is set to 220 m (from digitising gully lengths on digitised aerial photographs); and *T* is set to 100 years.

4.1.5 Bank erosion

SedNetNZ represents bank erosion at the reach-scale where the river network is divided into stream links based on the River Environment Classification (REC). The total mass of material eroded from riverbanks each year is a function of bank height, reach length, and bank migration rate (Dymond et al. 2016):

$$B_j = \rho M_j H_j L_j \tag{11}$$

where B_j is the total eroded mass for the jth stream link (t y^{-1}), ρ is the bulk density of the bank material (t m^{-3}), M_j is the bank migration rate (m y^{-1}), H_j is the mean bank height (m) and L_j is the length (m) of the jth stream link. Bank height is derived from a regional relationship with mean annual discharge and bulk density is estimated at 1.5 t m^{-3} (Dymond et al. 2016).

The predicted mass of material eroded from riverbanks represents the gross contribution of sediment supplied to the river channel per year. This does not account for redeposition and storage of eroded bank material on banks, within the channel bed or the lateral accretion of material on bars with channel migration. Hence, net bank erosion in SedNetNZ is estimated as one-fifth of gross bank erosion based on results from the Waipaoa River catchment (De Rose & Basher 2011). Overbank vertical accretion of fine sediment on floodplains beyond the active channel is represented separately (Dymond et al. 2016).

Bank migration rate (M_j) in equation 11 is represented as a function of six factors as follows:

$$M_j = SP_j Sn_j T_j V_j \left(1 - PR_j\right)\left(1 - PW_j\right) \tag{12}$$

where M_j is the bank migration rate (m y^{-1}) of the j-th stream link, SP_j is the stream power of the mean annual flood for the j-th stream link, Sn_j is the channel sinuosity rate factor of the j-th link, T_j is the soil texture-based erodibility factor of the j-th link, V_j is the valley confinement factor of the j-th link, PR_j is the proportion of riparian woody vegetation of the j-th link, and PW_j is the fraction of bank protection works for the j-th link (Smith et al. 2019a).

Stream power (SP_j) for the mean annual flood (MAF_j, m^3 s^{-1}) is estimated for each stream link by the product of mean annual flood and channel slope (S_j). MAF is estimated from a fitted power relationship ($MAF = aq^b$) with mean annual discharge (q, m^3 s^{-1}) using data from long-term river flow gauging within the catchment or region of interest:

$$SP_j = MAF_j S_j = a{q_j}^b S_j \tag{13}$$

Various studies report increasing bank migration rates with increasing bankfull discharge and stream power (Hooke 1979; Nanson & Hickin 1986; Walker & Rutherfurd 1999; Alber & Piégay 2017). While MAF has been shown to relate to bank erosion rates (Dymond et al. 2016), other factors, such as channel sinuosity (Nanson & Hicken 1983), the cohesiveness of bank materials (Julian & Torres, 2006), valley confinement (Hall et al. 2007), and riparian woody vegetation (Abernethy & Rutherfurd 2000), are also important, resulting in high levels of spatial variability in bank erosion.

We use the log-normal probability density function to represent the relationship between channel sinuosity and migration rate, which we term the sinuosity rate factor. This function allows us to represent the positive-skew observed in the relationship between channel sinuosity and migration rate (Crosato 2009). The dimensionless channel sinuosity rate factor (Sn_j) is calculated as

$$Sn_j = \frac{1}{(Sinu_j - 1)\sigma\sqrt{2\pi}}\, e^{\left(-\frac{(ln\,(Sinu_j - 1) - \mu)^2}{2\,\sigma^2}\right)} \tag{14}$$

where $Sinu_j$ is sinuosity of the j-th stream link of the REC2 network, and μ and σ are the mean and standard deviation parameters that determine the location and scale of the distribution. The μ and σ parameters are fitted using measurements of reach-scale bank migration rates.

The texture of bank material influences bank migration rates (Hickin & Nanson 1984; Julian & Torres 2006; Wynn & Mostaghini 2006). Our approach is based on an empirical relationship between percent silt + clay content (SC) and soil critical shear stress (τ_c) derived by Julian and Torres (2006) using data from Dunn (1959) as follows:

$$\tau_c = 0.1 + 0.1779SC + 0.0028SC^2 - 0.0000234SC^3 \quad (15)$$

SC is obtained from spatial data on soil textural classes compiled from the Fundamental Soil Layers (FSL) (Newsome et al. 2008), which provide national coverage. The soil texture-based erodibility factor (T_j) is represented by a power function to characterise the relationship between τ_c and bank erodibility for the j-th stream link:

$$T_j = c{\tau_{c,j}}^{-d} \quad (16)$$

where the c and d parameters are fitted using available bank migration rate data. The choice of a power function is based on experimental (Arulanandan et al. 1980) and field (Hanson & Simon 2001; Julian & Torres 2006) observations of the relationship between stream bank or bed critical shear stress and erodibility.

Floodplain extent and the level of valley confinement are factors that may limit lateral bank migration (Hall et al. 2007; De Rose & Basher 2011). The presence of steep valley sides and/or exposure of bedrock influence spatial patterns of erosion and deposition (Fryirs et al. 2016). Here, we adapt the Australian SedNet model approach to estimate a valley confinement factor (V_j) by using the mean slope (SB_j) in degrees of a buffer zone (4 × 15 m DEM pixel width) either side of the j-th stream link:

$$V_j = \left(1 - e^{\left(-15/SB_j\right)}\right)^{11} \quad (17)$$

Woody riparian vegetation typically increases bank stability via the effects of root reinforcement and root cohesion (Abernethy & Rutherfurd 2000; Hubble et al. 2010; Polvi et al. 2014; Konsoer et al. 2015). Woody vegetation can also increase roughness and flow resistance, thereby reducing the boundary shear stress acting on the bank surface (Thorne 1990). In addition, woody vegetation has hydrological effects on bank stability. For example, woody vegetation was found to be more effective than grass cover in lowering soil water content due to increased canopy interception and evapotranspiration, thus improving bank stability (Simon & Collinson 2002).

We represent the effect of riparian woody vegetation (PR_j) in reducing bank migration rates at the reach scale. Bank migration rates are reduced proportionally to the extent of woody riparian vegetation along the j-th stream link (equation 12). Stream links with complete riparian woody vegetation cover are assumed to erode at 0.05 of the migration rate with no woody cover (De Rose et al. 2003). Spatial information on woody vegetation is obtained from satellite imagery and intersected with the Land Information New Zealand (LINZ) digital stream network obtained from 1:50,000 topographic mapping. The mapped stream network was used in preference to the DEM-derived channel network because it tends to exhibit better planform accuracy which should improve spatial correspondence between channel position and riparian woody vegetation.

In some cases, the LINZ stream network provides poor representation of channel width for wider reaches with exposed gravel. To address this issue, the spatial union of the LINZ river polygons with LCDB v5 'river' and 'gravel and rock' land cover classes was used to produce revised river polygons. Mapped 'gravel and rock' areas located beyond the extent of the channel network were removed. The revised stream network layer improved alignment between channel banks and mapped woody vegetation when quantifying the reach-scale extent of riparian woody vegetation cover. The proportion of riparian woody vegetation is computed from the intersection of the revised stream network with a 15-m buffer and a classified map of 2002 woody vegetation cover (called EcoSat Woody) derived from Landsat TM at 15-m resolution (Dymond & Shepherd 2004).

We also include representation of channel protection works (PW_j) that are designed to reduce bank erosion (e.g. rock riprap, willow edge protection) as well as stopbanks employed for flood protection, where such data are available. We assume that over the multi-decadal model timescale, erosion mitigation would ultimately be targeted to where migrating riverbanks approach stopbanks, or that such interventions have already been implemented to protect stopbank integrity. The proportional length of bank erosion control measures (PEC_j) and stopbanks (PSB_j) is summed to give the proportion of channel works (PW_j) for the j-th stream link. PEC_j is computed as the length of erosion control measures within a stream link relative to the total length of that link. This assumes erosion control measures are targeted to the eroding bank side. Stopbanks may be located on either side of the channel irrespective of the direction of bank migration. Therefore, PSB_j is computed as the length of stopbanks in a link relative to 2 × link length.

Inputs to the bank erosion model component of SedNetNZ were obtained from national-scale spatial datasets comprising the REC2 and LINZ stream networks, 15-m DEM, FSL for soil data, and EcoSat Woody for 2002 woody vegetation cover. LCDBv5 was not used, despite being more recent because it has a minimum mapping unit of 10,000 m^2 versus 225 m^2 for EcoSat. This makes LCDB less suitable for characterising narrow corridors of woody vegetation often found along channel banks.

Hydrological data were provided by TRC. This comprises flow data from 20 gauging stations with records >10 years in length from across the region. These data were used to fit a relationship (Fig. 1) between mean annual discharge and mean annual flood ($MAF = 34q^{0.9}$, R^2 = 0.83) for use in calculating stream power for each REC2 link in the stream network. TRC also provided spatial data on stopbanks and channel protection works that have been included in the model simulations.

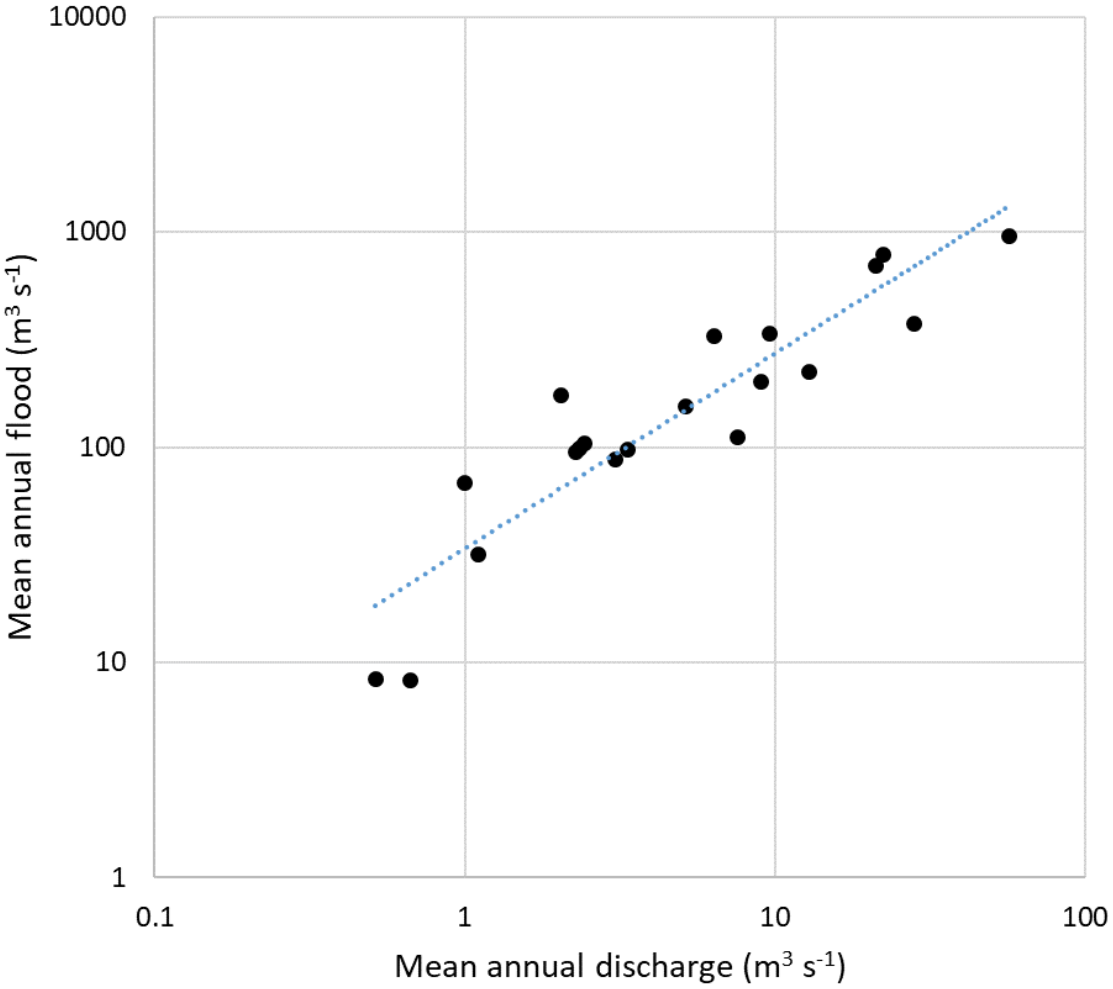


Figure 1. Fitted power relationship between mean annual discharge and mean annual flood (MAF) based on data from 20 gauging stations across Taranaki.

In the absence of mapped reach-scale channel changes within the Taranaki region, we used a combined dataset comprising measured bank migration rates from the Manawatu and Kaipara catchments to calibrate the bank erosion model (Spiekermann et al. 2017; Smith et al. 2019a). This calibration dataset has also been used in other recent applications of SedNetNZ in Hawke's Bay (Smith et al. 2020) and Southland (Smith et al. 2019b; Neverman et al. 2020). Calibration of the bank migration model was performed by minimising the mean square error (MSE) between predicted and observed data by optimising parameter values for the sinuosity (μ and σ) and bank soil texture (c and d) factors in equations 13 and 15, respectively. This produced reasonable agreement between measured and observed bank migration rates (Smith et al. 2019a; Fig. 2).

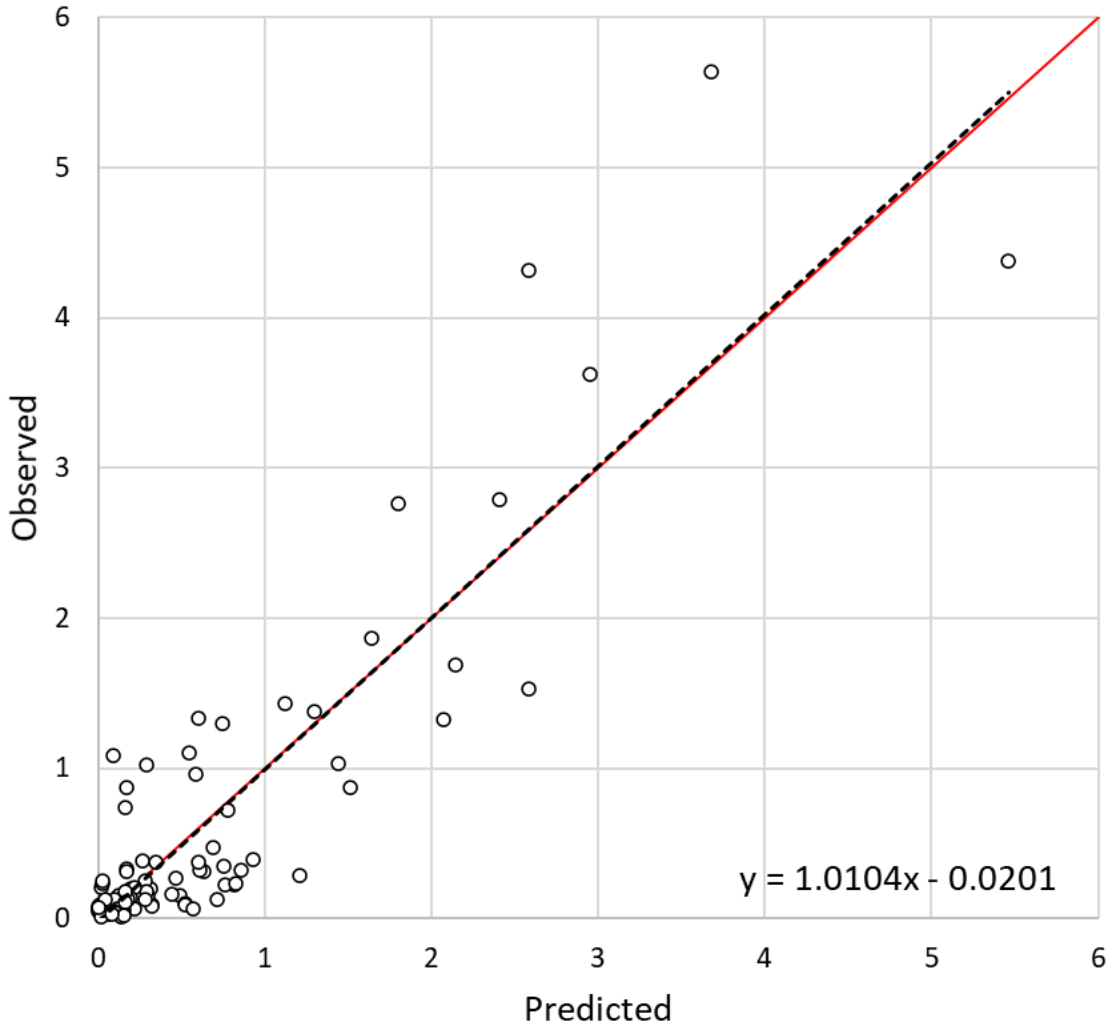


Figure 2. Plot comparing predicted versus observed bank migration rates (m y^{-1}) based on calibrated parameter values for the sinuosity and erodibility factors (Smith et al. 2019a). Fitted regression line (black dashed) and the 1:1 line (red) are also shown.

4.1.6 Sediment routing

SedNetNZ accounts for the deposition of sediment in lakes and on floodplains as the sediment is transported through the channel network.

To account for sediment trapping through lakes, we apply a revised SedNetNZ sediment routing algorithm. The revised routing algorithm applies a lake-specific sediment passing factor (*SPF*) to the net routed sediment load at the end of a REC2 sub-catchment draining to a lake. *SPF* was calculated using an adaptation of Gill's (1979) approximation of Brune's (1953) trap efficiency (the inverse of passing factor) curve for medium sediment:

$$SPF = 1 - \frac{V/I}{1.02(V/I) + 0.012} \quad (18)$$

where V is the lake volume and I is the annual inflow to the lake. This is similar to the approach of Hicks et al. (2019).

The mass of sediment deposited on the floodplain in a given reach is calculated as:

$$F_i = \left(\frac{pS_t}{\sum L_i S_i}\right) L_i S_i \quad (19)$$

where F_i is the total floodplain deposition (t y^{-1}) in the ith sub-catchment, p is the proportion of the catchment total sediment per sea-draining catchment that is deposited on floodplains in the catchment, set to 5% based on previous SedNetNZ parameterisation work carried out in the Manawatu (Dymond et al. 2016), S_t is the total sediment (t y^{-1}) per sea-draining catchment, L_i is the reach length (m) of floodplain per sub-catchment (as determined from Erosion Terrains), S_i is the total sediment (t y^{-1}) per sub-catchment.

4.2 Model simulations

The area modelled for this report comprises the REC2 sub-catchments within the four TRC Freshwater Management Units (FMUs). The FMUs were merged to create two aggregated FMUs for differential application of the modelling ruleset as outlined below: a hill country FMU defined as FMU D with inclusion of the Lake Rotokare Scenic Reserve, and a ringplain and coastal FMU comprised of FMU A, B, and C (Fig. 3). The difference in application of soil conservation between the aggregated FMUs was the limit of riparian fencing to third order and greater sub-catchments in the hill country FMU vs all sub-catchments in the ringplain and coastal FMU.

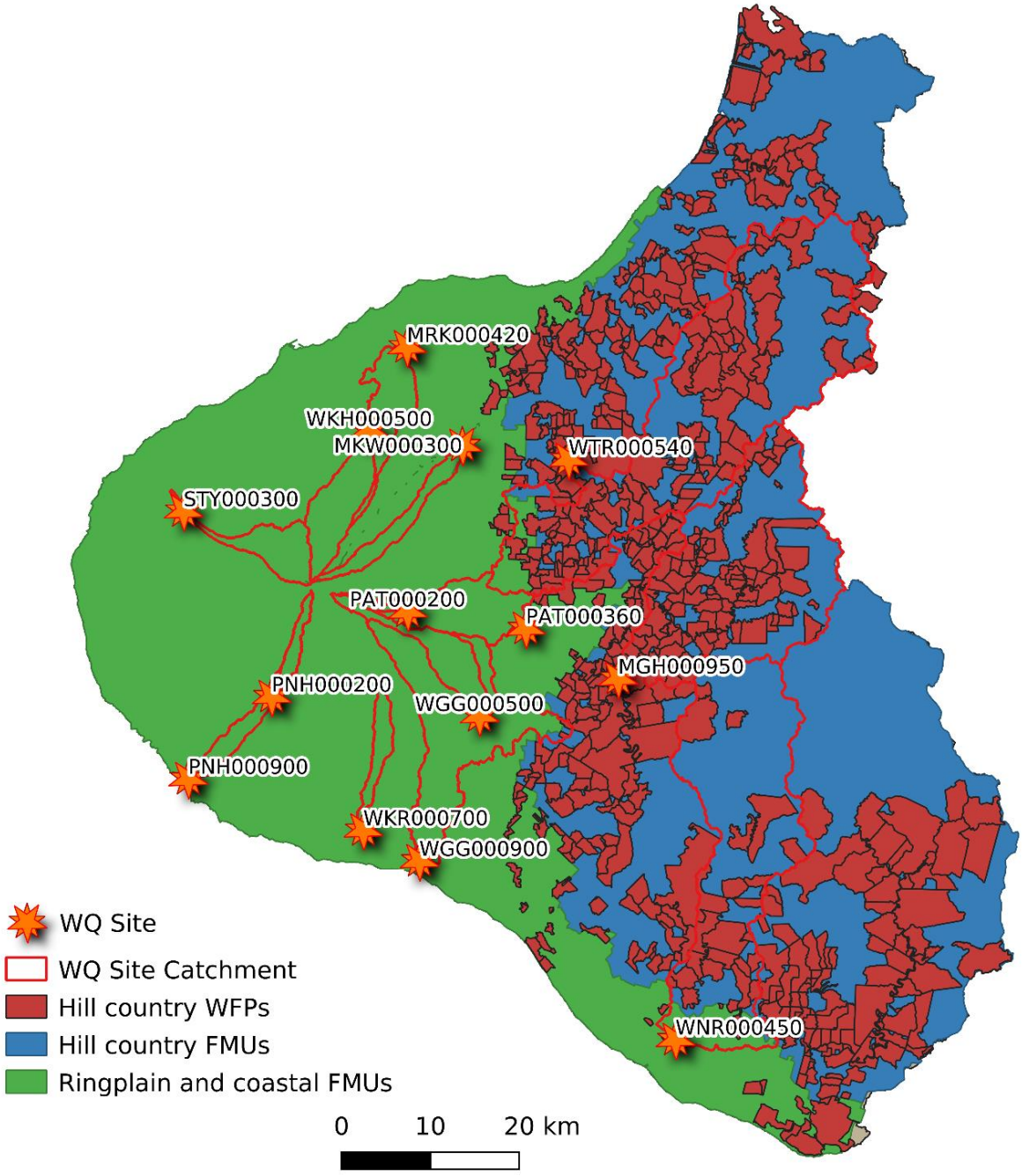


Figure 3. Distribution of hill country Whole Farm Plans and aggregated hill country and ringplain FMUs.

SedNetNZ model simulations were completed for the region as follows:

a An initial baseline using 1996 land cover (LCDBv1) without specific representation of soil conservation works, representing a pre-mitigation state.

b Contemporary baseline using 2018 land cover (LCDBv5) with representation of TRC conservation works completed to date and their estimated maturity, representing the contemporary state.

c Future soil conservation scenario with fully matured and implemented conservation works comprising a) farm plans in hill country areas and b) riparian fencing in 3rd order and greater hill country channels, and all ring plain and coastal channels (see Fig. 3), representing a future state under best practice soil conservation works.

4.2.1 Hill country farm plans

Whole Farm Plans are represented spatially in the model using data provided by TRC. Hill country WFPs (Figure 3) have soil conservation works consisting of a combination of space-planted trees on non-G class slopes, and scrub reversion on G class slopes (identified from farm-scale LUC data provided by TRC) applied to appropriate pasture areas within the farm. It was assumed that WFPs were fully implemented in the year the plan was setup, as recorded in the dataset provided by TRC, following the method used by Basher et al (2020), McDowell et al (2020), Monaghan et al (2021), and Neverman et al (2019). This provided an age for the trees and scrub, calculated for 2018.

The erosion reduction effectiveness for fully matured space-planted trees (≥15 years old) is modelled as 70%, and for fully matured scrub reversion (≥10 years old) is modelled as 90%, and applied to mass-movement erosion processes, following Dymond et al. (2016).

As some WFPs were younger than 15 years in 2018, the contemporary baseline scenario modelled the erosion reduction effectives of trees and scrub as a function of their age using a maturity factor:

$$M_f = \frac{2018 - Y}{15} \tag{20}$$

where M_f is the maturity factor of the WFP in 2018, and Y is the year WFP mitigations were fully implemented (Basher et al 2020; McDowell et al 2020; Monaghan et al 2021; Neverman et al 2019).

4.2.2 Riparian fencing

Riparian fencing is represented spatially in the model using data supplied by TRC. Fencing data was classified by TRC as 'existing', 'completed' or 'proposed'. We applied the following ruleset to determine how the fencing data was used in each model simulation:

a. Initial baseline	• Only mapped fencing classed as 'existing' was included.
b. Contemporary baseline	• Mapped fencing classed as 'existing' and 'completed' were used. Comparison with the initial baseline simulation shows the reduction in bank erosion achieved by the riparian fencing completed to date.
c. Future conservation scenario	• Riparian fencing was applied to a) all stream orders within ring plain and coastal FMUs and b) ≥3rd order streams within predominantly hill country FMUs in addition to mapped 'existing' and 'completed' fences included in the contemporary baseline simulation. • The additional fencing was applied to areas deemed 'mitigatable' (i.e. streams on agricultural land) and excluded from 'non-mitigatable' areas (e.g. native forest on conservation estate) for each REC2 stream link.

We applied a 60-m buffer to the REC2 stream network and used this to select those fences in the vicinity of channels. This buffer is designed to accommodate variations in channel width as well as positional error evident in REC2 stream segments relative to mapped fence lines. The length of selected fences was summed per REC2 stream link and used in determining the effect of fencing on bank erosion.

We estimate the fraction of stream link that has been fenced (FR_j) as the length of fence relative to 2 x stream link length, which approximates the maximum extent of fencing when present on both sides of a channel for a given REC2 reach. The reduced net suspended sediment load from bank erosion due to fencing and stock exclusion (B_{F_j}) is computed using equation 21, as follows:

$$B_{F_j} = B_j \times \left(1 - 0.8FR_j\right) \quad (21)$$

where B_j is the net suspended sediment load from bank erosion without the effect of fences reducing erosion. A reduction of 80% in net suspended sediment load from bank erosion may be attributable to riparian fencing and stock exclusion (Dymond et al. 2016). This reflects the effect of reduced stock trampling and foraging on banks (Trimble 1994) as well as the potential for riparian woody vegetation to become better established in the absence of livestock over the longer-term.

4.3 Contemporary and achievable attribute states

The 5-year median visual clarity was calculated for 14 water quality monitoring sites using the most recent black disc measurements (n = 60). This allows the contemporary fine suspended sediment attribute state to be identified for each site from the NPS-FM 2020 based on sediment class[2] and median visual clarity (Table 1).

[2] Suspended sediment classes for the REC2 network are available at https://data.mfe.govt.nz/layer/103687-hydrological-modelling-to-support-proposed-sediment-attribute-impact-testing-2020/

Table 1. Attribute bands and numeric attribute states for fine suspended sediment. Reproduced from Table 8 in the NPS-FM 2020

Attribute band and description	Numeric attribute state by suspended sediment class (visual clarity(m))			
	1	2	3	4
A Minimal impact of suspended sediment on instream biota. Ecological communities are similar to those observed in natural reference conditions.	≥1.78	≥0.93	≥2.95	≥1.38
B Low to moderate impact of suspended sediment on instream biota. Abundance of sensitive fish species may be reduced.	<1.78 and ≥1.55	<0.93 and ≥0.76	<2.95 and ≥2.57	<1.38 and ≥1.17
C Moderate to high impact of suspended sediment on instream biota. Sensitive fish species may be lost.	<1.55 and >1.34	<0.76 and >0.61	<2.57 and >2.22	<1.17 and >0.98
National bottom line	1.34	0.61	2.22	0.98
D High impact of suspended sediment on instream biota. Ecological communities are significantly altered, and sensitive fish and macroinvertebrate species are lost or at high risk of being lost.	<1.34	<0.61	<2.22	<0.98

The relationships between required reductions in median visual clarity and mean annual suspended sediment loads developed by Dymond et al. (2017) and simplified by Hicks et al. (2019) were used to calculate the reductions in mean annual suspended sediment loads required to achieve the NPS-FM 2020 attribute bands at each water quality monitoring site. The proportional reduction in load required to achieve each attribute band is calculated as a function of the difference between the baseline and minimum numeric attribute state for each band:

$$PR_v = 1 - (V_o/V_b)^{1/a} \quad (22)$$

where PR_v is the minimum proportional reduction in load required to achieve the attribute state, V_o is the minimum visual clarity for each band, V_b is the baseline median visual clarity, and a was assumed to take the national average reported by Hicks et al. (2019) as –0.76.

Given the national bottom-line threshold overlaps with the bottom of the range for band C, our analysis looks at reductions required to meet the national bottom line, band B, and band A. Achieving band C requires only a marginal increase in load reduction from that required to achieve the national bottom line.

To identify which attribute band a water quality monitoring site would fall in to after existing soil conservation works mature and riparian fencing is completed, the reduction in mean annual load between the contemporary baseline and future conservation scenarios was compared to the required load reduction to achieve each attribute band. Where the achieved reduction was higher than the required load reduction, the associated attribute band is considered achievable.

5 Results

5.1 Scenario mean annual suspended sediment loads

Mean annual suspended sediment loads are presented for the Taranaki region in Table 2 and visualised in Figure 1, and for the water quality monitoring sites in Table 3. To visualise the distribution of erosion rates, net specific sediment yield (t km^2 yr^{-1}) is presented in Figure 2 by REC2 sub-catchment across the region for each scenario.

Table 2. Total mean annual suspended sediment loads for the Taranaki region under each modelled scenario

Scenario	Mean annual suspended sediment load (Mt yr^{-1})
Initial Baseline	2.38
Contemporary Baseline	1.68
Future conservation works	1.44

Table 3. Total mean annual suspended sediment loads at water quality monitoring sites under each modelled scenario, rounded to significant figures

Site Code	Location	Initial baseline suspended sediment load (t yr^{-1})	Contemporary baseline suspended sediment load (t yr^{-1})	Future scenario mean annual suspended sediment load (t yr^{-1})
MGH000950	Mangaehu River at Raupuha Rd Bridge	369,600	231,300	195,600
MKW000300	Maketawa Stream at Tarata Rd	1,200	670	650
MRK000420	Mangaoraka Stream at Corbett Rd	1,000	760	660
PAT000200	Patea River at Barclay Rd Bridge	170	150	150
PAT000360	Patea River at Skinner Rd Bridge	2,700	2,000	1,600
PNH000200	Punehu Stream at Wiremu Rd	750	560	550
PNH000900	Punehu Stream at SH45	1,700	1,000	960
STY000300	Hangatahua (Stony) River at Mangatete Rd	8,900	8,300	8,300
WGG000500	Waingongoro River at Eltham Rd Bridge	2,200	1,900	1,900
WGG000900	Waingongoro River at SH45	13,300	9,200	8,500
WKH000500	Waiwhakaiho River at SH3	4,300	3,700	3,500
WNR000450	Whenuakura River at Nicholson Rd	194,000	144,400	135,500
WTR000540	Waitara River at Autawa Rd	539,000	345,500	292,600
WKR000700	Waiokura pumphouse	130	100	90

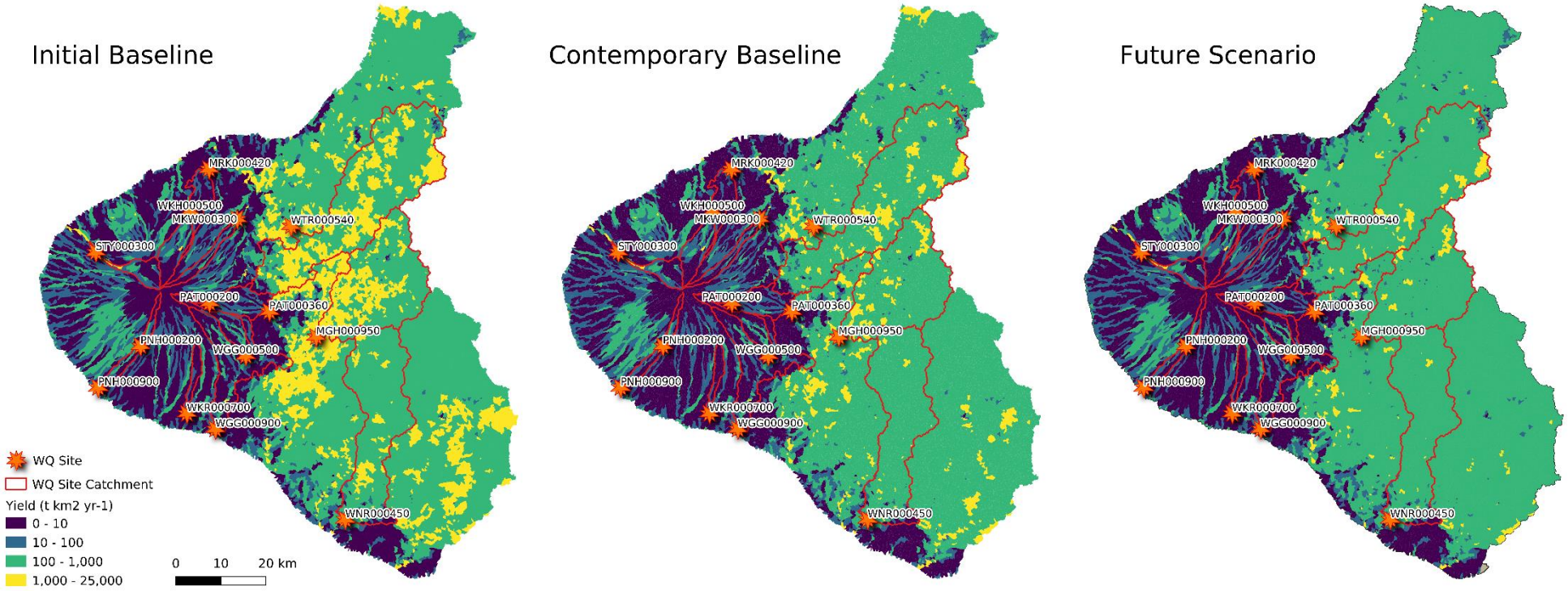


Figure 4. Net suspended sediment yield (t km^2 yr^{-1}) for the REC2 sub-catchments for each scenario.

5.2 Reductions in load

A 29% reduction in load is seen across the region between the initial and contemporary baseline scenarios (Table 4). This is a result of changing landcover (which caused an increase in load in some reaches) between 1996 and 2018, and the implementation and maturity of WFPs and riparian fencing. A 15% reduction in load is seen across the region between the contemporary and future conservation scenarios, resulting from maturing of soil conservation works, and completion of riparian fencing. A 40% reduction is seen between the initial baseline and future conservation scenario.

Table 4. Regional changes in mean annual suspended sediment load between scenarios, rounded to significant figures

Scenarios	Absolute change (t yr^{-1})	Proportional change
Initial baseline to contemporary baseline	–698,000	–29%
Initial baseline to future mitigation	–947,000	–40%
Contemporary baseline to future mitigation	–249,000	–15%

At the water quality monitoring sites, reductions are seen at all sites between the initial and contemporary baseline scenarios, and at all but one site between the contemporary baseline and future mitigations scenario (Table 5). The local net load reductions achievable within the water quality monitoring site catchments between the contemporary baseline and future conservation scenario are shown in Figure 4.

Table 5. Absolute and proportional reductions in mean annual suspended sediment load between modelled scenarios at water quality monitoring sites

Site Code	Location	Initial baseline to contemporary baseline	Initial baseline to future scenario	Contemporary baseline to future scenario
MGH000950	Mangaehu River at Raupuha Rd Bridge	138,330 (37%)	173,957 (47%)	35,627 (15%)
MKW000300	Maketawa Stream at Tarata Rd	556 (45%)	581 (47%)	25 (4%)
MRK000420	Mangaoraka Stream at Corbett Rd	302 (28%)	399 (38%)	97 (13%)
PAT000200	Patea River at Barclay Rd Bridge	20 (12%)	20 (12%)	0 (0%)
PAT000360	Patea River at Skinner Rd Bridge	682 (25%)	1,082 (40%)	400 (20%)
PNH000200	Punehu Stream at Wiremu Rd	180 (24%)	194 (26%)	14 (2%)
PNH000900	Punehu Stream at SH45	720 (42%)	744 (44%)	25 (3%)
STY000300	Hangatahua (Stony) River at Mangatete Rd	542 (6%)	559 (6%)	17 (0.2%)
WGG000500	Waingongoro River at Eltham Rd Bridge	243 (11%)	272 (13%)	29 (2%)
WGG000900	Waingongoro River at SH45	4,128 (31%)	4,791 (36%)	663 (7%)
WKH000500	Waiwhakaiho River at SH3	660 (15%)	876 (20%)	216 (6%)
WNR000450	Whenuakura River at Nicholson Rd	49,682 (26%)	58,619 (30%)	8,937 (6%)
WTR000540	Waitara River at Autawa Rd	193,572 (36%)	246,494 (46%)	52,921 (15%)
WKR000700	Waiokura pumphouse	28 (22%)	37 (29%)	9 (9%)

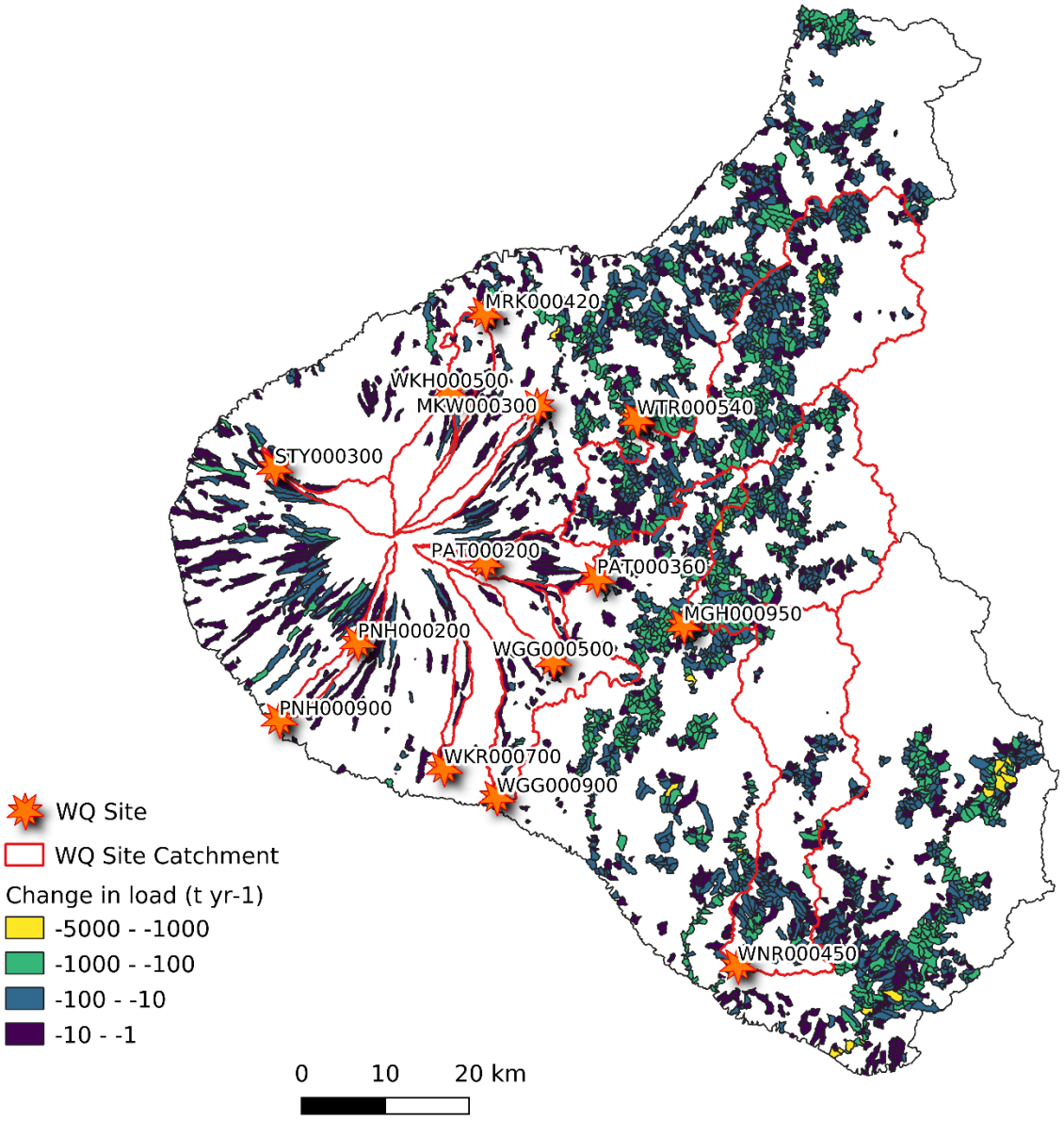


Figure 5. Achievable load reductions (t yr^{-1}) in each REC2 sub-catchment between the contemporary baseline and future conservation scenarios.

5.3 Suspended sediment attribute states

The contemporary attribute band for each water quality monitoring site based on the NPS-FM 2020 are presented in Table 6 and Figure 6. Of the 14 monitoring sites assessed, seven are in band A (highest achievable state), two are in band B, two are band C, and three do not achieve the national bottom line (band D).

Table 6. Baseline visual clarity and attribute state at water quality monitoring sites. Baseline visual clarity was calculated as the median of the most recent 5 years (60 samples) of monthly monitoring data.

Site Code	Location	NPS-FM 2020 sediment class	Baseline visual clarity (m)	Contemporary attribute band
MGH000950	Mangaehu River at Raupuha Rd Bridge	4	1.075	C
MKW000300	Maketawa Stream at Tarata Rd	1	2.1	A
MRK000420	Mangaoraka Stream at Corbett Rd	1	2.1	A
PAT000200	Patea River at Barclay Rd Bridge	1	4.045	A
PAT000360	Patea River at Skinner Rd Bridge	1	1.975	A
PNH000200	Punehu Stream at Wiremu Rd	1	1.7	B
PNH000900	Punehu Stream at SH45	1	1.6	B
STY000300	Hangatahua (Stony) River at Mangatete Rd	1	2.335	A
WGG000500	Waingongoro River at Eltham Rd Bridge	1	1.79	A
WGG000900	Waingongoro River at SH45	1	1.42	C
WKH000500	Waiwhakaiho River at SH3	1	3.205	A
WNR000450	Whenuakura River at Nicholson Rd	2	0.32	D
WTR000540	Waitara River at Autawa Rd	2	0.4	D
WKR000700	Waiokura pumphouse	1	0.67	D

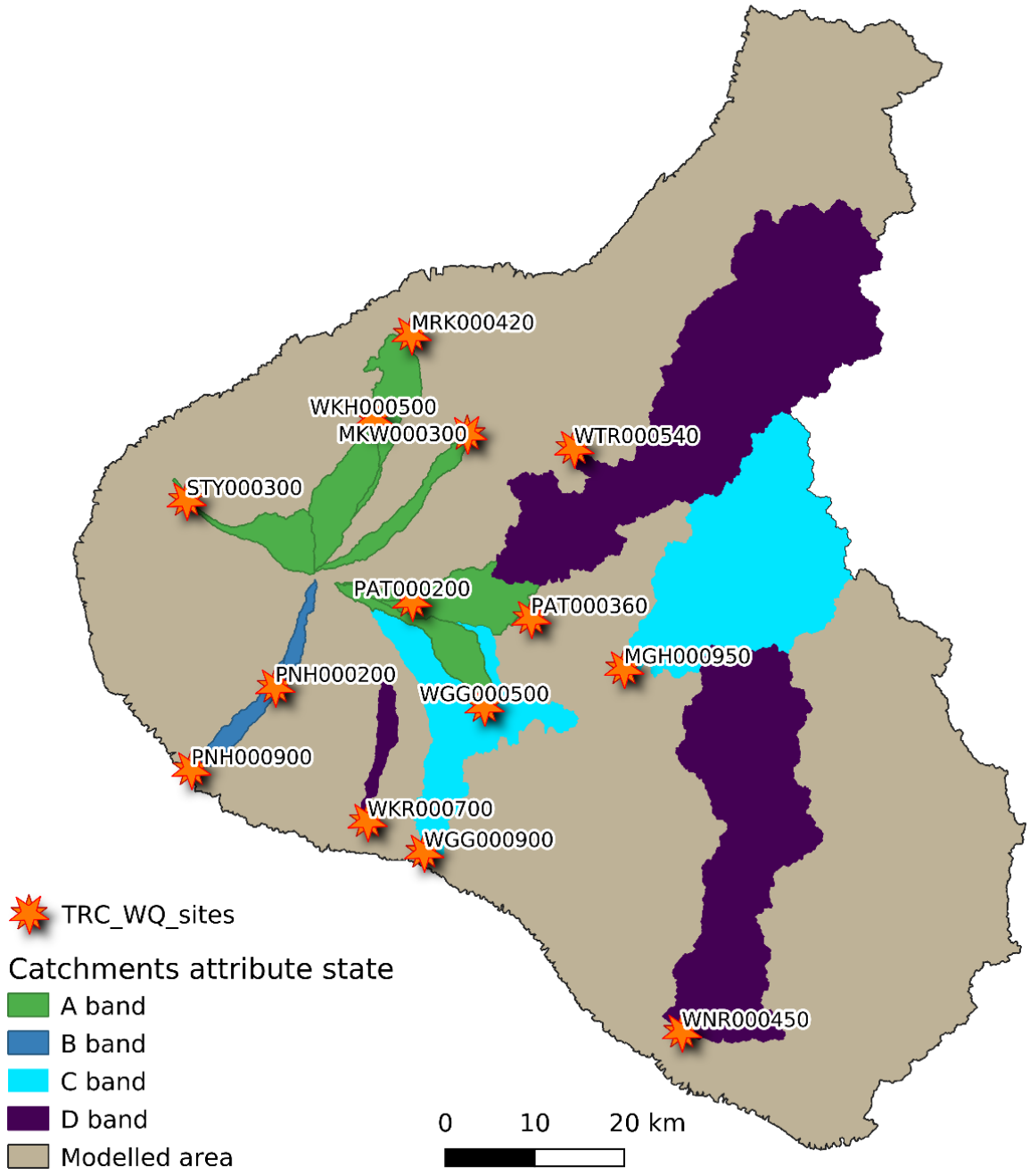


Figure 6. Contemporary attribute state of the 14 water quality monitoring sites.

5.4 Achievement of NPS-FM 2020 suspended sediment attribute states

The proportional and absolute reductions in load required for water quality monitoring sites to achieve each attribute band are presented in Table 7. Where the reduction is zero, the band is already achieved. Based on the reduction in load achieved between the contemporary baseline and future mitigation scenarios, the ability of soil conservation works to achieve each attribute state at water quality monitoring sites is presented in Table 8. The SedNetNZ data layer accompanying this report can be used to rank sub-catchments from highest to lowest achievable reductions within each water quality monitoring catchment, and identify farms associated with the sub-catchments to prioritise for soil conservation works.

Table 7. Proportional and absolute reductions in mean annual suspended sediment load required to achieve NPS-FM 2020 attribute states at water quality monitoring sites, round to significant figures

Site Code	Location	Proportion reduction in load required			Absolute reduction in load required (t yr^{-1})		
		National bottom line	B band	A band	National bottom line	B band	A band
MGH000950	Mangaehu River at Raupuha Rd Bridge	0%	11%	28%	0	28,300	75,200
MKW000300	Maketawa Stream at Tarata Rd	0%	0%	0%	0	0	0
MRK000420	Mangaoraka Stream at Corbett Rd	0%	0%	0%	0	0	0
PAT000200	Patea River at Barclay Rd Bridge	0%	0%	0%	0	0	0
PAT000360	Patea River at Skinner Rd Bridge	0%	0%	0%	0	0	0
PNH000200	Punehu Stream at Wiremu Rd	0%	0%	6%	0	0	30
PNH000900	Punehu Stream at SH45	0%	0%	13%	0	0	130
STY000300	Hangatahua (Stony) River at Mangatete Rd	0%	0%	0%	0	0	0
WGG000500	Waingongoro River at Eltham Rd Bridge	0%	0%	0%	0	0	0
WGG000900	Waingongoro River at SH45	0%	11%	26%	0	1,000	2,300
WKH000500	Waiwhakaiho River at SH3	0%	0%	0%	0	0	0
WNR000450	Whenuakura River at Nicholson Rd	57%	68%	75%	99,800	118,600	131,600
WTR000540	Waitara River at Autawa Rd	43%	57%	67%	167,700	224,500	264,000
WKR000700	Waiokura pumphouse	60%	67%	72%	60	67	72

Table 8. Achievable load reductions (t yr^{-1}) at the WQ sites between the contemporary baseline and future conservation scenarios, rounded to significant figures

Site Code	Location	Load reduction achievable (t/yr^{-1})	Load reduction achievable (%)	Achievable attribute state
MGH000950	Mangaehu River at Raupuha Rd Bridge	27,300	15%	B
MKW000300	Maketawa Stream at Tarata Rd	30	4%	A
MRK000420	Mangaoraka Stream at Corbett Rd	100	13%	A
PAT000200	Patea River at Barclay Rd Bridge	0	0%	A
PAT000360	Patea River at Skinner Rd Bridge	400	20%	A
PNH000200	Punehu Stream at Wiremu Rd	10	2%	B
PNH000900	Punehu Stream at SH45	25	3%	B
STY000300	Hangatahua (Stony) River at Mangatete Rd	20	0.2%	A
WGG000500	Waingongoro River at Eltham Rd Bridge	30	2%	A
WGG000900	Waingongoro River at SH45	660	7%	C
WKH000500	Waiwhakaiho River at SH3	200	6%	A
WNR000450	Whenuakura River at Nicholson Rd	4,400	6%	D
WTR000540	Waitara River at Autawa Rd	46,200	15%	D
WKR000700	Waiokura pumphouse	10	9%	D

6 Discussion

6.1 Effectiveness of soil conservation works

A significant reduction in mean annual suspended sediment loads has been achieved across the region since Whole Farm Plans were established, with a 29% (698,000 t yr^{-1}) net reduction in modelled load between the initial and contemporary baseline scenarios. A further reduction of 249,000 (15%) t yr^{-1} is estimated to be achievable once existing soil conservation works reach full maturity, and riparian fencing is completed across the region, giving a total net reduction of 947,000 t yr^{-1} (40%) between the initial baseline and future mitigation scenario.

Contemporary reductions in suspended sediment load range from 6 to 45% at water quality monitoring sites since WFPs were established. Lower reductions are projected between the contemporary baseline and future mitigation scenarios at all sites (0.2 – 20%) due to the estimated maturity of WFPs and extent of riparian fencing being high in the contemporary baseline, therefore leaving less room for improvement in the future. However, it is possible we have overestimated the maturity of WFPs in the contemporary scenario, and there may therefore be more room for maturing of soil conservation works in the future, thus achieving greater reductions than estimated here.

This analysis excludes any consideration of the likely impact of climate change in increasing erosion rates and sediment loads. Basher et al. (2020) modelled the effect of erosion mitigation and climate change on sediment loads in the Manawatu-Whanganui region and suggested that the increase in sediment load resulting from climate change impacts may exceed the reductions achieved by land management by 2090. This may have significant implications for sediment management policy.

6.2 Attribute bands

Seven of the 14 water quality monitoring sites are presently in the A band under the NPS-FM 2020. This is the highest achievable standard. Two sites are in band B, and two in band C. These bands are above the national bottom line (minimum standard) and therefore do not require further reductions. Three sites (WNR000450, WTR000540, and WKR000700) sit below the national bottom line. Of the seven sites below band A, only the Mangaehu is predicted to see an improvement in attribute state under the future scenario. The inability to achieve the reductions required to meet the national bottom line may result from a combination of factors. First, the reductions required in load for these sites are significant as their visual clarity is well below the national bottom line. To achieve the reductions needed to meet the national bottom line would require a significant proportion of the catchment to be available for future soil conservation works. However, a significant proportion of the catchment area is already woody vegetation as per LCDBv5, and the majority of hill country pasture in the catchments has an existing farm plan, and the maturity of these farm plans is relatively high in the contemporary scenario. Thus, there is relatively little room for further soil conservation works or increasing effectiveness of existing works through maturation. Given their high proportion of woody land cover, these catchments could be considered to have naturally high levels of erosion and therefore sediment loads. The NPS-FM 2020 does allow for flexibility in visual clarity targets for sites affected by naturally occurring processes which contribute to high sediment loads, such as in naturally highly coloured brown-water streams. The sites at WNR000450, WTR000540, and WKR000700 may fall within this category.

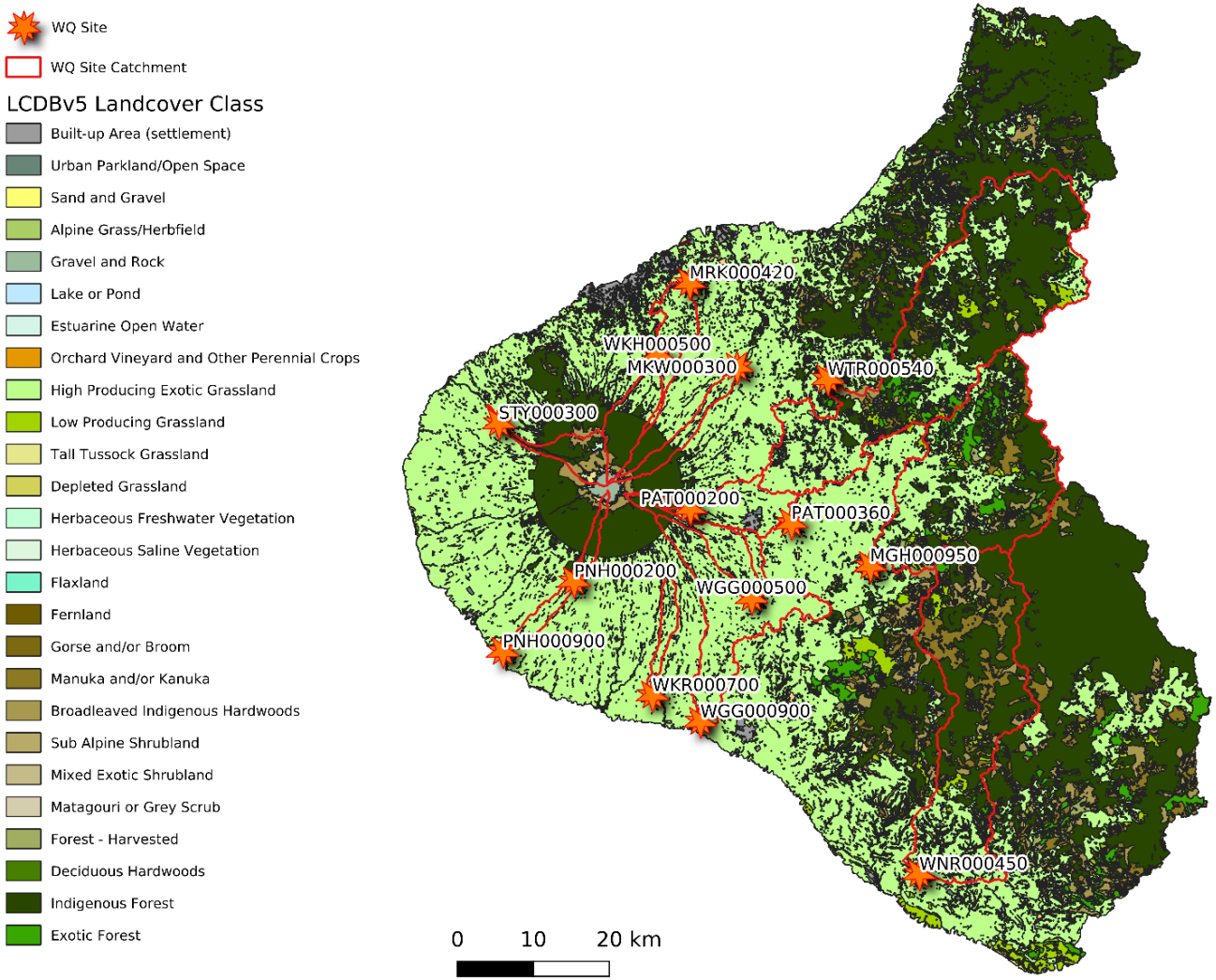


Figure 7. Land cover as represented by LCDBv5.

6.3 Model assumptions and limitations

There are several limitations in SedNetNZ modelling of baseline loads, and in the calculation of the load reductions required to meet NPS-FM 2020 fine suspended sediment attribute states. We outline these limitations in terms of each modelling component below. Model outputs should be interpreted in the context of these limitations.

6.3.1 Surficial erosion

The key limitations in the surficial erosion component of SedNetNZ relate to the calculation of the *C* and *K* factors in the NZUSLE, and the availability of suitable input data. We have improved the calculation of the *K* factor within the Taranaki region by utilising FSL data to compute a spatially variable *K* factor instead of the uniform *K* factor previously used in the NZUSLE (e.g. Dymond et al. 2016). Higher resolution soils data from the region, such as S-map, may improve estimates of surficial erosion for Taranaki.

6.3.2 Shallow landslide erosion

In the absence of regional multi-temporal data on shallow landslide occurrence, it was necessary to use data from other regions to calibrate the landslide component of SedNetNZ for the Taranaki region. Calibration data from the Manawatu (Dymond et al. 2016) was used to define the slope thresholds for landslide occurrence and density. *f(s)* was therefore adjusted using information on storm rainfall magnitude-frequency (NIWA HIRDS v4) and estimated landslide triggering rainfall thresholds (Basher et al. 2020).

Regional multi-temporal mapping of shallow landslides would enable better parametrisation of the shallow landslide component of SedNetNZ and, combined with regional LiDAR data, would enable better spatial representation of slope thresholds for shallow landslide initiation and density.

6.3.3 Earthflow and Gully erosion

Both earthflow and gully erosion are represented in SedNetNZ using a spatial averaging approach based on estimated presence and spatial extent of these erosion features in the Erosion Terrains layer, and their erosion rate is uniform (Dymond et al. 2016). It is therefore possible that earthflow and gully erosion may be represented in sub-catchments that do not contain these features, or may not be represented where they are present. Spatial variation in erosion rates between individual earthflow or gully features is also not captured. Future modelling could benefit from individual erosion feature mapping to enable more accurate spatial representation across the region and further data collection on erosion rates.

6.3.4 Riverbank erosion

There are several limitations related to the revised bank erosion component that require consideration when analysing results at the sub-catchment scale. In the absence of local data on riverbank migration rates, it was necessary to calibrate the bank migration model

using available measurements from the Manawatu and Kaipara catchments in the North Island. We recognise this potentially introduces additional and unquantified error into model predictions for Taranaki catchments due to differences in catchment geology and channel planform. However, the dataset from Manawatu and Kaipara does span a large range in observed bank migration rates, riparian woody vegetation extents, soil textures, channel slope, and sinuosity variables for the mapped reaches (Spiekermann et al. 2017; Smith et al. 2019a).

Representation of riparian woody vegetation has been derived from EcoSat Woody (Dymond & Shepard 2004) as LCDB is less suitable for representing narrow strips of riparian corridor. Predictions of bank migration rates are therefore based on woody vegetation presence/absence in 2002. A further challenge results from the spatial correspondence of mapped channel location and woody vegetation resulting from the alignment of REC2 to the channel, and changes in channel planform since mapping occurred. Availability of catchment-wide LiDAR data would enable improved spatial representation of riparian woody vegetation and coherence with channel locations.

6.3.5 Soil conservation works

Modelling of soil conservation works assumes all existing Whole Farm Plans include space-planted trees on all appropriate land, and these trees have been planted at the recommended density to achieve a 70% reduction in erosion, and there is no mortality. It also assumes all G class slopes have been reverted.

Hawley and Dymond (1988) reported that space-planting does not always achieve a 70% reduction in hillslope erosion due to mortality of trees and/or ineffective tree spacing.

When accounting for the maturity of these space-planted trees and scrub reversion, we assume all mitigatable land was planted or retired during the year the WFP was established; however, planting may have been phased over a number of years, or not undertaken. There is therefore some uncertainty about the maturity and effectiveness of existing WFPs in 2018. It is also possible some space-planting or scrub reversion has occurred on farms that is not captured in the existing WFP data used in this modelling, or in LCDBv5. If this is the case, baseline loads in catchments where this occurs may be underestimated here. The model may therefore underestimate what further reductions are achievable from baseline, although this is likely to be minor.

6.3.6 Load reductions and achievable attribute states

Mean annual suspended sediment load reductions to achieve visual clarity attribute states were estimated using equations developed by Hicks et al. (2019) from simplifications in the relationships reported by Dymond et al. (2017). The key assumption for calculating required load reductions to meet attribute states is the relationship between sediment load and flow remain constant at a site. In reality, this relationship may change due to changes in catchment hydrology, leading to changes in the relationship between a given flow and suspended sediment concentration (Hicks et al. 2019). As data are not presently available to predict these changes, we assume that the associated relationships remain constant.

We have also estimated the required load reductions using empirical models fitted to a national dataset. This should result in the models being fitted to a wide range of catchment variables and therefore representing the variability across Taranaki, and sites from Taranaki were used in the national dataset (see Hicks et al. 2019), but this may lead to under- or over-estimation of required reductions at any one site. This relationship does not account for the local variability in the relationship between sediment load and visual clarity that arises due to variations in the sediment characteristics that affect the optical properties of flows between sites, such as the presence of fine-grained clay minerals (Hicks et al. 2019). Future improvements could be made by locally calibrating the relationship between visual clarity and sediment loads at the assessment sites.

It is also important to consider that visual clarity baseline attribute states are derived from monthly fixed interval sampling. This sampling likely results in visual clarity being mostly measured at or near baseflow, when the majority of the sediment load may be derived from within-channel sources (e.g. remobilisation from channel bed or from bank erosion). In contrast, the modelled mean annual sediment loads reflect storm event-driven erosion and sediment loads, where shallow landslide erosion is a dominant sediment source in hill country areas of Taranaki over multi-decadal timescales. There may therefore be some disconnect between the sediment sources reduced by soil conservation works and those that contribute to fixed-interval visual clarity samples (while acknowledging that some storm-derived hillslope sediment may enter channel bed storage where it could undergo subsequent remobilisation during lower flows).

6.3.7 Riparian fencing

It is assumed that any fence segment in the vicinity of the buffered REC2 stream links are in place to exclude stock, and that woody vegetation can establish in the area between the fence and channel. This approach is complicated by the potential misalignment of the REC2 network and the true channel location, which is particularly challenging in low order streams. This may lead to incorrect fencing lengths at any given REC2 segment. However, this approach is spatially explicit, and is a better spatial representation of existing stock exclusion than the regionally uniform estimate used by Neverman et al. (2019), and therefore better represents the spatial variation in the effect of pre-existing mitigations, particularly at larger scales. Future modelling could benefit from the inclusion of an attribute field in fencing databases to demarcate those fences providing stock exclusion from riparian areas.

7 Conclusions

SedNetNZ modelling for the Taranaki region suggests soil conservation works implemented since ~1996 have resulted in a 29% net reduction in mean annual suspended sediment loads across the region. As existing soil conservation works mature, and further riparian fencing is completed, a further 15% reduction is expected across the region under the current landcover configuration.

Based on the past 5 years of monthly water quality monitoring data from 14 sites across the region, seven of the 14 sites presently sit in the A band for suspended sediment in the NPS-FM 2020. This is the highest achievable attribute state. Of the remaining seven sites, only the Mangaehu is predicted to see an improvement in attribute state under the future scenario, moving from band C to band B. Four of these sites are above the national bottom line so do not require further reductions. Three sites presently fall below the national bottom line for visual clarity in the NPS-FM 2020. The inability to achieve the reductions required to meet the national bottom line may result from a combination of factors, including overestimation of the contemporary effectiveness of soil conservation works in the model, limiting the room for future improvement, or the naturally occurring high rates of erosion in the catchments which could be naturally highly coloured streams, and therefore may warrant some reduction in their bottom line from that of the national bottom line for their sediment class.

8 Recommendations

- One of the key limitations of the analysis presented in this report is the assumption of soil conservation maturity based on the establishment date of Whole Farm Plans, and the assumption that WFPs are fully implemented in their first year. This may result in an over estimation of the maturity and effectiveness of trees for erosion reduction in the contemporary baseline scenario, resulting in an underestimation of achievable load reductions in the future scenario. Data for each farm plan detailing the degree of implementation to date (i.e. proportion of planned tree planting that has been undertaken) and the maturity of implemented works would improve our estimation of contemporary reductions, and room for further reduction.
- While a timeline has not been explicitly given for full effectiveness of soil conservation works to take effect, it is likely to be several decades as recent space-planted trees and retired land reach full maturity. It is possible that climate change may result in an increase in loads despite conservation works by the end of the century (Basher et al. 2020). Future work could look at modelling the potential impact of climate change on sediment loads in the Taranaki region using SedNetNZ and implications for meeting NPS-FM (2020) sediment attribute targets.
- Availability of S-Map data for Taranaki would enable better representation of soil parameters in the surficial erosion component of SedNetNZ.
- The availability of regional LiDAR data will enable better representation of erosion processes within SedNetNZ. Future work could update SedNetNZ modelling for the region when LiDAR data become available.

- Building a regional multi-temporal shallow landslide database would enable better calibration of the shallow landslide component in future applications of SedNetNZ in the Taranaki region.

9 Acknowledgements

We thank Taranaki Regional Council for funding this work. We acknowledge staff from Taranaki Regional Council, particularly Don Shearman, Gary Bedford, and Damon McGhie for discussions leading to this piece of work and provision of data. We thank Chris Philips for reviewing this report.

10 References

Abernethy B, Rutherfurd ID 2000. The effect of riparian tree roots on the mass-stability of riverbanks. Earth Surface Processes and Landforms 25: 921–937.

Alber A, Piégay H 2017. Characterizing and modelling river channel migration rates at a regional scale: case study of south-east France. Journal of Environmental Management 202: 479–493.

Arulanandan K, Gillogley E, Tully R 1980. Development of a quantitative method to predict critical shear stress and rate of erosion of natural undisturbed cohesive soils. USACE, Waterways Experiment Station Technical Report GL-80-5. Vicksburg, MS: USACE.

Basher L, Spiekermann R, Dymond J, Herzig A, Hayman E, Ausseil AG 2020. Modelling the effect of land management interventions and climate change on sediment loads in the Manawatū–Whanganui region. New Zealand Journal of Marine and Freshwater Research 2020 54: 490–511.

Betts H, Basher L, Dymond J, Herzig A, Marden M, Phillips C 2017. Development of a landslide component for a sediment budget model. Environmental Modelling & Software 92: 28–39.

Brune GM 1953. Trap efficiency of reservoirs. Eos, Transactions American Geophysical Union 34: 407–18.

Byrd RH, Lu P, Nocedal J, Zhu C 1995. A limited memory algorithm for bound constrained optimization. SIAM Journal on Scientific Computing 16: 1190–1208.

Crosato A 2009. Physical explanations of variations in river meander migration rates from model comparison. Earth Surface Processes and Landforms 34: 2078–2086.

DeRose RC 2013. Slope control on the frequency distribution of shallow landslides and associated soil properties, North Island, New Zealand. Earth Surface Processes and Landforms 38: 356–371.

De Rose R, Basher LR 2011. Measurement of river bank and cliff erosion from sequential LiDAR and historical aerial photography. Geomorphology 126: 132–147.

De Rose R, Prosser IP, Weisse M, Hughes AO 2003. Patterns of erosion and sediment and nutrient transport in the Murray-Darling Basin. CSIRO Land and Water Technical Report 32/03.

Desmet PJJ, Govers G. 1996. A GIS procedure for automatically calculating the USLE LS factor on topographically complex landscape units. Journal of Soil and Water Conservation 51(5): 427–433.

Duncan MJ, Woods RA 2013. Water regulation. In Dymond JR ed. Ecosystem services in New Zealand – conditions and trends. Lincoln: Manaaki Whenua Press.

Dunn IS 1959. Tractive resistance of cohesive channels. Journal of the Soil Mechanics and Foundations Division 85: 1–24.

Dymond JR, Betts HD, Schierlitz CS 2010. An erosion model for evaluating regional land-use scenarios. Environmental Modelling and Software 25: 289–298.

Dymond, JR, Davies-Colley, RJ, Hughes, AO, Matthaei, CD 2017. Predicting improved optical water quality in rivers resulting from soil conservation actions on land. Science of the Total Environment 603–604: 584–592.

Dymond JR, Herzig A, Basher L, Betts HD, Marden M, Phillips CJ, Ausseil AE, Palmer DJ, Clark M, Roygard J 2016. Development of a New Zealand SedNet model for assessment of catchment-wide soil-conservation works. Geomorphology 257: 85–93.

Dymond JR, Jessen MR, Lovell LR 1999. Computer simulation of shallow landsliding in New Zealand hill country. International Journal of Applied Earth Observation and Geoinformation 122–131.

Dymond JR, Shepherd JD 2004. The spatial distribution of indigenous forest and its composition in the Wellington region, New Zealand, from ETM+ satellite imagery. Remote Sensing of Environment 90: 116–125.

Eyles GO 1983. The distribution and severity of present soil erosion in New Zealand. New Zealand Geographer 39: 12–28.

Foster GR, Meyer LD, Onstad CA 1977. A runoff erosivity factor and variable slope length exponents for soil loss estimates. Transactions of the ASAE 20: 683–687.

Franklin P, Stoffells R, Clapcott J, Booker D, Wagenhoff A, Hickey C 2019. Deriving potential fine sediment attribute thresholds for the National Objectives Framework. NIWA Client Report No: 2019039HN prepared for Ministry for the Environment.

Fryirs KA, Wheaton JM, Brierley GJ 2016. An approach for measuring confinement and assessing the influence of valley setting on river forms and processes. Earth Surface Processes & Landforms 41: 701–710.

Gill MA 1979. Sedimentation and useful life of reservoirs. Journal of Hydrology 44: 89–95.

Guy GG 1977. Landslide investigations, Main North Line Railway, South Island, New Zealand. Unpublished MSc thesis, University of Canterbury. http://ir.canterbury.ac.nz/handle/10092/8095

Hall JE, Holzer DM, Beechie TJ 2007. Predicting river floodplain and lateral channel migration for salmon habitat conservation. Journal of the American Water Resources Association 43: 786–797.

Hanson GJ, Simon A 2001. Erodibility of cohesive streambeds in the loess area of the midwestern USA. Hydrological Processes 15: 23–38.

Hawley JG, Dymond JR 1988. By how much do trees reduce landsliding? Journal of Soil and Water Conservation 43: 495–498.

Hickin EJ, Nanson GC 1984. Lateral migration rates of river bends. Journal of Hydraulic Engineering 110: 1557–1567.

Hicks M, Haddadchi A, Whitehead A, Shankar U, 2019. Sediment load reductions to meet suspended and deposited sediment thresholds. NIWA Client Report 2019100CH prepared for Ministry for the Environment.

Hicks DM, Shankar U, McKerchar AI, Basher L, Jessen M, Lynn I, Page M 2011. Suspended sediment yields from New Zealand rivers. Journal of Hydrology (NZ) 50: 81–142.

Hooke JM 1979. An analysis of the processes of river bank erosion. Journal of Hydrology 42: 39–62.

Hubble TCT, Docker BB, Rutherfurd ID 2010. The role of riparian trees in maintaining riverbank stability: a review of Australian experience and practice. Ecological Engineering 36: 292–304.

Hughes AO 2016. Riparian management and stream bank erosion in New Zealand. New Zealand Journal of Marine and Freshwater Research 50: 277–290.

Julian JP, Torres R 2006. Hydraulic erosion of cohesive riverbanks. Geomorphology 76: 193–206.

Konsoer KM, Rhoads BL, Langendoen EJ, Best JL, Ursic ME, Abad JD, Garcia MH 2015. Spatial variability in bank resistance to erosion on a large meandering, mixed bedrock-alluvial river. Geomorphology 252: 80–97.

Marden M, Phillips CJ, Rowan D 2008. Recurrent displacement of a forested earthflow and implications for forestmanagement, East Coast Region, New Zealand. IAHS Publications 325: 491–501.

Marden M, Herzig A, Basher L 2014. Erosion process contribution to sediment yield before and after the establishment of exotic forest: Waipaoa catchment, New Zealand. Geomorphology 226: 162–174.

McCool DK, Foster GR, Mutchler CK, Meyer LD 1989. Revised slope length factor for the Universal Soil Loss Equation. Transactions of the ASA 32: 1571-76.

McDowell RW, Monaghan RM, Smith C, Manderson A, Basher L, Burger DF, Laurenson S, Pletnyakov P, Spiekermann, Depree C 2020. Quantifying contaminant losses to water from pastoral land uses in New Zealand III. What could be achieved by 2035? New Zealand Journal of Agricultural Research 0: 1–21.

Midgley TL, Fox GA, Heeren DM. 2012. Evaluation of the bank stability and toe erosion model (BSTEM) for predicting lateral retreat on composite streambanks. Geomorphology 145–146: 107–114.

Monaghan R, Manderson A, Basher L, Spiekermann R, Dymond J, Smith C, Muirhead R, Burger D, McDowell R 2021. Quantifying contaminant losses to water from pastoral landuses in New Zealand II. The effects of some farm mitigation actions over the past two decades. New Zealand Journal of Agricultural Research 0: 1–25.

Nanson GC, Hicken EJ 1983. Channel migration and incision on the Beatton River. Journal of Hydraulic Engineering 109: 327–337.

Nanson GC, Hickin EJ 1986. A statistical analysis of bank erosion and channel migration in western Canada. Geological Society of America Bulletin 97: 497–504.

Neverman AJ, Djanibekov U, Soliman T, Walsh P, Spiekermann R, Basher L 2019. Impact testing of a proposed suspended sediment attribute: identifying erosion and sediment control mitigations to meet proposed sediment attribute bottom lines and the costs and benefits of those mitigations. Manaaki Whenua – Landcare Research Contract Report LC3574 prepared for Ministry for the Environment.

Neverman A, Smith HG, Herzig A, Basher L (2020) Modelling baseline suspended sediment loads and load reductions required to achieve Draft Freshwater Objectives for Southland. Landcare Research Contract Report LC3749 prepared for Environment Southland.

Newsome PFJ, Wilde RH, Willoughby EJ 2008. Land resource information system spatial data layers: data dictionary. Palmerston North, Landcare Research New Zealand Ltd. http://digitallibrary.landcareresearch.co.nz/cdm/ref/collection/p20022coll14/id/67

Page MJ, Trustrum NA, Dymond JR 1994. Sediment budget to assess the geomorphic effect of a cyclonic storm, New Zealand. Geomorphology 9: 169–88.

Polvi LE, Wohl E, Merritt DM 2014. Modeling the functional influence of vegetation type on streambank cohesion. Earth Surface Processes & Landforms 39: 1245–1258.

Reid LM, Page MJ 2003. Magnitude and frequency of landsliding in a large New Zealand catchment. Geomorphology 49: 71–88.

Renard, KG, 1997. Predicting soil erosion by water: a guide to conservation planning with the Revised Universal Soil Loss Equation (RUSLE). Washington DC: United States Government Printing.

Rosewell CJ, Loch RJ 2002. Estimation of the RUSLE soil erodibility factor. In: McKenzie N, Coughlan K, Cresswell H eds Soil physical measurement and interpretation for land evaluation. Melbourne, Australia: CSIRO Publishing.

Simon A, Collinson AJC 2002. Quantifying the mechanical and hydrologic effects of riparian vegetation on streambank stability. Earth Surface Processes & Landforms 27: 527–546.

Smith HG, Spiekermann R, Dymond J, Basher L 2019a. Predicting spatial patterns in riverbank erosion for catchment sediment budgets. New Zealand Journal of Marine and Freshwater Management 53: 338–362.

Smith HG, Herzig A, Dymond J, Basher L 2019b. Application of a revised SedNetNZ model to the Oreti and Aparima catchments, Southland. Manaaki Whenua – Landcare Research Contract Report LC3507 prepared for Our Land and Water National Science Challenge.

Smith HG, Spiekermann R, Betts H, Neverman AJ 2021. Comparing methods of landslide data acquisition and susceptibility modelling: Examples from New Zealand. Geomorphology :107660.

Smith HG, Spiekermann R, Herzig A, Dymond J 2020. Application of a revised bank erosion model to update SedNetNZ results for Hawke's Bay. Landcare Research Contract Report LC3740 prepared for Hawke's Bay Regional Council.

Spiekermann R, Betts H, Dymond J, Basher L 2017. Volumetric measurement of riverbank erosion from sequential historical aerial photography. Geomorphology 296: 193–208.

Thorne CR 1990. Effects of vegetation on riverbank erosion and stability. In: Thornes JB ed. Vegetation and erosion. Chichester UK: John Wiley & Sons. Pp. 125–144.

Trimble SW 1994. Erosional effects of cattle on streambanks in Tennessee, U.S.A. Earth Surface Process & Landforms 19: 451–464.

Walker M, Rutherfurd ID 1999. An approach to predicting rates of bend migration in meandering alluvial streams. In Rutherfurd ID, Bartley R eds Proceedings of the Second Australian Stream Management Conference. Melbourne, Australia: Cooperative Research Centre for Catchment Hydrology. Pp. 659–665.

Wang G, Gertner G, Xianzhong L, Anderson A 2001.Uncertainty assessment of soil erodibility factor for revised universal soil loss equation. Catena 46: 1–14.

Wischmeier WH, Johnson CB, Cross BV 1971. Soil erodibility nomograph for farmland and construction sites. Journal of Soil and Water Conservation 26: 189193.

Woods R, Hendrikx J, Henderson R, Tait A. 2006. Estimating mean flow of New Zealand rivers. Journal of Hydrology (NZ) 45: 95–110.

Wyn T, Mostaghimi S 2006. The effects of vegetation and soil type on streambank erosion, southwestern Virginia, USA. Journal of the American Water Resources Association 42: 69–82.

Yang X, Gray J, Chapman G, Zhu Q, Tulau M, McInnes-Clarke S 2018. Digital mapping of soil erodibility for water erosion in New South Wales, Australia. Soil Research 56: 15870.

Zhang X, Phillips C, Pearce A 1991. Surface movement in an earthflow complex, Raukumara Peninsula, New Zealand. Geomorphology 4: 261–27